Trends in Applied Sciences Research

ISSN 1819-3579

Academic
Journals Inc.

www.academicjournals.com

Trends in Applied Sciences Research 1 (1): 25-40, 2006
ISSN 1819-3579

Finite Element Modeling of Adhesively Bonded Joints

[1]K.G. Muthurajan, [2]K. Sankaranarayanasamy,
[3]S.B. Tiwari and B. Nageswara Rao
[1]Faculty of Mechanical Engineering,
National Engineering College, Kovilpatti-628503, India
[2]Faculty of Mechanical Engineering,
National Institute of Technology, Tiruchirappalli-620015, India
[3]Structural Analysis and Testing Group,
Vikram Sarabhai Space Centre, Trivandrum-695022, India

Abstract: Finite element analysis for adhesively bonded joints has been carried out by developing a special 6 node isoparametric element for the adhesive layer. The adhesive layer is assumed to be relatively thin and behaves elastically as simple tension-compression springs and shear spring connecting the adherends. The results of a metal-metal single lap joint are found to be in good agreement with the closed-form solution of Goland and Reissner. This adhesive element can be utilized for modeling adhesively bonded joints having shaped adherends for optimum joint efficiency.

Key words: Adherend, adhesive, single lap joint, aluminium, steel, boron/epoxy, normal stress, shear stress

Introduction

Joints in components or structures incur a weight penalty, are a source of failure and cause manufacturing problems; whenever possible, therefore, a designer will avoid using them. Unfortunately it is rarely possible to produce a construction without joints owing to limitations on material size, convenience in manufacture or transportation and the need for access in order to inspect or repair the structure (Mathews and Rawlings, 1999).

Developments in the application of advanced composites in vehicle design involve material systems utilizing composites bonded to metallic structural members. These hybrid composites combine the high tensile capacity of a composite with the shear strength of a metal to obtain a structurally efficient and cost effective component. Applications have included horizontal stabilizers of aircraft, tail sections of helicopters and high speed ground transportations vehicles. Basically, there are two types of joint commonly employed with composite materials: adhesively bonded joints and mechanically fastened joints. Welding is also a possibility for thermoplastic composites, but this technique is not well developed for load-carrying joints (Mathews *et al*., 2000). The joining of structural components by adhesive bonding is extremely desirable, because both bolting and riveting result in the cutting of fibres as well as the introduction of stress concentrations, of a more severe magnitude than for a bonded joint. Bonded joints can be made by bonding (gluing) together pre-cured

Corresponding Author: B. Nageswara Rao, Structural Analysis and Testing Group,
Vikram Sarabhai Space Centre, Trivandrum-695022, India
Tel: +91 471 2565831 Fax: +91 471 2564181

laminates with a suitable adhesive or by forming joints during the manufacturing process, in which case the joint and the laminate are cured at the same time (co-cured or co-bonded). A joint represents a discontinuity in a structure and the resulting high stresses often initiate failure.

State of the Art

To extend the use of composites as reinforcing elements in vehicular structures, the transfer of stress between the composite and the metallic substrate must be understood. There are many publications concerned with the stress analysis of bonded joints and analyses have been carried out for various joint configurations and for different properties of the adherends and adhesives. Results have been obtained in closed-form or from numerical analyses.

Goland and Reissner (1944) were among the first of several investigators to analyze the single lap joint configuration. They determined approximate stress state in the adhesive layer as a function of geometric parameters and elastic properties of the adhesive and adherends, which were confirmed later by Carpenter (1989). Erdogan and Ratwani (1971) developed a differential equation for a multi-step scarf joint between dissimilar equal thickness axially aligned adherends. Chang and Muki (1974) analyzed single lap joints between similar and dissimilar adherends completely ignoring any adhesive layer that might exist. They used integral transform techniques and reduced the problem to the solution of a pair of Fredholm integral equations. Numerical results were given for stress intensity factors for identical adherends of varying adherend thickness/lap length.

Hart-Smith (1973a, 1973b, 1973c, 1974) considered the effect of adhesive ductility on the strength of lap and butt joints. He modeled the ductility by elastic-plastic behavior with three parameters. The elastic-plastic parameters are fixed such that maximum shear strain, shear stress and shear strain energy of the model are matched to their true values. This idealization gives accurately the maximum capacity strength of long joints. Yuceoglu and Updike (1980) have carried out the stress analysis of bonded plates and joints. However, the shaping of the adherends was found to have a strong effect on the shear stress distribution in the adhesive considered by Ramamurthy and Rao (1978). Many of these analytical solutions are valid only for special cases of geometry, material and loading conditions.

Barker and Hatt (1973) developed a special element to represent the thin adhesive layer as a degenerate case of a rectangular element. This represents the tension shear springs very effectively. Reddy and Sinha (1975) have applied the finite element methods to the stress analysis of adhesive bonded joints.

Standard finite elements may not always be well suited for the analysis of adhesive layers. It is normally observed that the adhesive layer is extremely thin compared with other dimensions of a bonded structure. It is also known that most elements give the best results when the aspect ratio of the width to the height of the element is approximately unity. Distorted elements have poor properties. It has been found that an element having a large aspect ratio becomes much stiffer in the transverse direction and much weaker in the axial direction. Motivated by the work of Barker and Hatt (1973) a special 6-noded isoparametric element is developed for the adhesive layer compatible with the general 8-noded isoparametric quadrilateral element (Zienkiewicz, 1971), which is used to idealize the adherends. The adhesive layers are assumed to be relatively thin and behave elastically as simple tension-compression springs and shear springs connecting the adherends. This implies that stress variation in the thickness direction through the adhesive layer is ignored and that only the transverse normal stress and the longitudinal shear stress in the adhesive layer influence equilibrium.

In the development of bonded joints for structures, a simple joint can be fabricated first and tested for its suitability in structures. The size of the joint can be first estimated from the knowledge of the part sizes to be joined, the allotted space for the joint and a general idea of how much overlap is required to carry the load. With such knowledge, the preliminary joint designs can be made that can be refined using an iterative analysis procedure. The finite element method is a powerful numerical tool that can be used to estimate the direct and shear stress distribution required in the failure analysis.

Finite element analysis has been carried on a single lap joint containing dissimilar isotropic or orthotropic adherends. There are two main reasons for this interest. Firstly a lap joint which consists of two most common joint designs employed in industry and secondly it is simple and convenient test geometry for evaluating adhesive joints. However, the stresses in the adhesive layer are not, in practice uniform and stress concentrations arise from the differential straining of the bonded substrate and form the eccentricity of the loading path.

Formulation

In the method of finite elements, the structure is divided into discrete parts, each of which has to be compatible in the force and displacement continuum with adjacent elements. By applying suitable boundary conditions, any form of the joint can be analyzed numerically by solving a series of equations of the form:

$$\{F\} = \{K\}\{\delta\} \tag{1}$$

where {F}is a vector of the nodal forces, {K}is a stiffness matrix composed from the elemental stiffness and {δ} is a vector of the resulting nodal displacement. The basic steps involved in the finite element method are: finite element idealization of the structure; evaluation of element stiffness by deriving nodal force-displacement relationships; Assemblage of the stiffness and force matrices for the system of elements and nodes; introduction of boundary conditions; solution of the resulting equations for nodal displacements; calculation of strains and stresses based on nodal displacements. An interpolation function or a shape function which has unit value at one nodal point and zero value at all other nodal points. When the geometry and displacements of the element are described in terms of the same parameters and are of the same order then these element are called isoparametric elements.

A numerical procedure for the analysis of two dimensional bonded joints is described here using quadratic isoparametric elements. Adherents are idealized by the 8-node isoparametric quadrilateral element, whereas the adhesive layer is modeled by the 6- node special element. Geometrical details of these elements are given in Fig. 1.

The geometry of the general element for adherends is represented by:

$$\begin{matrix} x \\ y \end{matrix} = \sum_{i=1}^{8} N_i(\xi,\eta) \begin{matrix} x_i \\ y_i \end{matrix} \tag{2}$$

where the shape functions, N_i (i = 1 to 8) are

$$N_i = \frac{1}{4}(1+\xi\xi_i)(1+\eta\eta_i)(\xi\xi_i+\eta\eta_i-1)+\frac{1}{2}(1-\xi^2)(1+\eta\eta_i)+\frac{1}{2}(1+\xi\xi_i)(1+\eta^2) \tag{3}$$

The two dimensional square element shown in Fig. 1, having local co-ordinates (ξ,η) with its boundaries defined by: $\eta=-1$, $\xi=1$, $\eta=1$, $\xi=-1$. (ξ_i,η_i) is a local coordinate for the node i in the eight node square element. The displacements (u, v) at any point in the element are defined by:

$$\begin{matrix} u \\ v \end{matrix} = \sum_{i=1}^{8} N_i(\xi,\eta) \begin{matrix} u_i \\ v_i \end{matrix} \tag{4}$$

The element strains are

$$\{\varepsilon\} = \left[\frac{\partial u}{\partial x}, \frac{\partial v}{\partial y}, \frac{\partial u}{\partial y} + \frac{\partial v}{\partial x}\right]^T = [B]\{\delta\}^e \tag{5}$$

where, [B] is the strain-shape function matrix. From Eq. 3 and 4, a part of the [B] matrix applicable to the ith node is given by:

$$B_i = \begin{matrix} \frac{\partial N_i}{\partial x} & 0 \\ 0 & \frac{\partial N_i}{\partial y} \\ \frac{\partial N_i}{\partial y} & \frac{\partial N_i}{\partial x} \end{matrix} = [J]^{-1} \begin{matrix} \frac{\partial N_i}{\partial \xi} & 0 \\ 0 & \frac{\partial N_i}{\partial \eta} \\ \frac{\partial N_i}{\partial \eta} & \frac{\partial N_i}{\partial \xi} \end{matrix} \tag{6}$$

where, [J] is the Jacobian matrix given by

$$[J] = \begin{matrix} \frac{\partial x}{\partial \xi} & \frac{\partial y}{\partial \xi} \\ \frac{\partial x}{\partial \eta} & \frac{\partial y}{\partial \eta} \end{matrix} \tag{7}$$

The general relationship between stresses and strains can be written as:

$$\{\sigma\} = \{\sigma_x \sigma_y \tau_{xy}\}^T = [D]\{\varepsilon\} - \{\varepsilon_i\} + \{\sigma_0\} \tag{8}$$

where, $\{\varepsilon_0\}$ are the initial strains and $\{\sigma_o\}$ are the initial stresses. [D] is the elasticity matrix for plane stress case given by:

$$[D] = \frac{E_x}{E_x - \nu_{xy}^2 E_y} \begin{matrix} E_x & \nu_{xy}E_y & 0 \\ \nu_{xy}E_y & E_y & 0 \\ 0 & 0 & \frac{(E_x - \nu_{xy}^2 E_y)G_{xy}}{E_x} \end{matrix} \tag{9}$$

Here E_x and E_y are modulus of elasticity, G_{xy} is the rigidity modulus in x-y plane and ν_{xy} is the Poisson's ratio.

The element stiffness is given by :

$$[K]^e = \int_A [B]^T[D][B]t \; dx \; dy \tag{10}$$

where, t is the thickness of the element.

Distributed loads at the edges of the elements and equivalent forces due to initial strains (such as thermal strains) are considered here. The nodal forces on an element under such loads are given by:

$$\{F\}^e = [K]^e\{\delta\}^e + \{F\}^e_q + \{F\}^e_b \tag{11}$$

where, $\{F\}^e_q$ is a vector of the equivalent nodal forces due to thermal strains and $\{F\}^e_q$ is a vector of the nodal forces due to distributed loads at the edges of the element.

The nodal forces due to distributed loading is given by:

$$\{F\}^e_b = -\int \{N\}^T\{g\}dx\, dy \tag{12}$$

where, $\{g\}$ is the distributed loading per unit area.

The initial strains can be computed from

$$\{F\}^e_q = -\int_A [B]^T[D]\{\varepsilon_0\}t\, dx\, dy \tag{13}$$

where, $\{\varepsilon_0\} = \{\alpha_x\ \alpha_y\ 0\}^t \Delta T$ for orthotropic materials in plane stress. α_x and α_y are the coefficients of thermal expansions in x and y directions, respectively and ΔT is the temperature change within the element.

Details on the 6-node special element for adhesive layer are given below. Since the adhesive layer is relatively thin, the special element used to idealize it assumes identical coordinates for the top and bottom nodes. In addition, the longitudinal direct stress and the variations of the other two stresses across the thickness of the adhesive layers are neglected.

The geometry of the element (which is a two dimensional curve) is represented by:

$$\begin{matrix} x \\ y \end{matrix} = \sum_{i=1}^{3} N_i(\xi) \begin{matrix} x_i \\ y_i \end{matrix} \tag{14}$$

where the shape functions, N_i(i=1,2,3) are given as:

$$N_i = \frac{1}{2}(1+\xi\xi_{si})\xi\xi_{si} + 1-\xi^2 \tag{15}$$

The local top and bottom layer displacements are given by:

$$\begin{matrix} u \\ v \end{matrix}^{top} = \sum_{i=1}^{3} N_i(\xi) \begin{matrix} u_{i+3} \\ v_{i+3} \end{matrix} \tag{16}$$

$$\begin{matrix} u \\ v \end{matrix}^{bottom} = \sum_{i=1}^{3} N_i(\xi) \begin{matrix} u_i \\ v_i \end{matrix} \tag{17}$$

The local normal and shear strains in the adhesive layer are defined by:

$$\varepsilon = (v^{top} - v^{bottom})/t_a \tag{18}$$

$$\gamma = (u^{top} - u^{bottom})/t_a \tag{19}$$

where t_a is the thickness of the adhesive element
The stiffness matrix for the adhesive element is:

$$[k]^e = t_a \int_{-1}^{1} [R]^T [B]^T [D]_a [B][R] \left(\frac{\partial x}{\partial \xi}^2 + \frac{\partial y}{\partial \xi}^2\right)^{\frac{1}{2}} d\xi \tag{20}$$

where, $[B] = \{-B_1 - B_2 - B_3\ B_1\ B_2\ B_3\}$

$$B_i = \begin{matrix} 0 & 0 \\ 0 & -N_i \\ N_i & 0 \end{matrix}, \tag{21}$$

$$[D]_a = \begin{matrix} 0 & 0 & 0 \\ 0 & E_a & 0 \\ 0 & 0 & G_a \end{matrix}, \tag{22}$$

$$[R] = \begin{matrix} s & 0 & 0 & 0 & 0 & 0 \\ 0 & s & 0 & 0 & 0 & 0 \\ 0 & 0 & s & 0 & 0 & 0 \\ 0 & 0 & 0 & s & 0 & 0 \\ 0 & 0 & 0 & 0 & s & 0 \\ 0 & 0 & 0 & 0 & 0 & s \end{matrix}, \tag{23}$$

$$s = \begin{matrix} \cos\theta & \sin\theta \\ -\sin\theta & \cos\theta \end{matrix}, \tag{24}$$

and,

$$\theta = \tan^{-1} \frac{\partial y}{\partial \xi} \Big/ \frac{\partial x}{\partial \xi} \tag{25}$$

E_a and G_a in Eq. 22 are the Young's modulus and the shear modulus of the adhesive layer.
While evaluating the integrals for the element stiffness matrix as well as equivalent nodal forces, all the Cartesian coordinates (x, y) system is converted to local coordinates (ξ,η) system through the determinant of Jacobian matrix. The following 3-point Gauss quadrature rule is used to evaluate the integrals

$$(...)dx\ dy = \int_{-1}^{+1}\int_{-1}^{+1} (...)\ \det[J]\ d\xi\ d\eta \tag{26}$$

Table 1: Mechanical properties of materials for adherends and adhesive layer

Material	E_{11} (G Pa)	E_{22} (G Pa)	ν_{21}	G_{12} (G Pa)
Aluminium	68.9	68.9	0.33	25.9
Steel	205.9	205.9	0.30	79.2
Boron	209.0	19.0	0.21	6.4
Adhesive	0.561	0.561	0.33	0.211

Table 2: Overall orthotropic properties of Boron/Epoxy laminate

Lay-up	E_{XX} (G Pa)	E_{YY} (G Pa)	ν_{XY}	G_{XY} (G Pa)
Angle-Ply				
[± 30]°	70.8	17.0	1.347	43.0
[± 45]°	23.1	23.1	0.805	55.2
[± 60]°	17.0	70.8	0.324	43.0
Quasi-isotropic				
[0/±45/90]°s	81.1	81.1	0.326	30.8

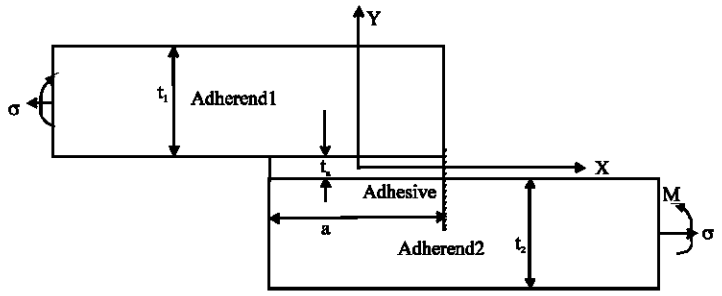

Fig. 1: Geometrical details of single of lap joint

Results and Discussion

To examine the adequacy of the developed six-node isoparametric element for the adhesive layer, a single lap metal-metal joint for which closed form solution available, is modeled here. The thicknesses of the adherends are: $t_1 = t_2 = 1.0$ mm. The overlap length, a = 4 mm. The origin of the reference is at the canter of the adhesive layer. The total length of single lap joint is 16 mm. Figure 3 shows the finite element idealization. A total of 70 eight-node iso-parametric quadrilateral elements for the two adherends and 10 special six-node iso-parametric elements for the adhesive layer and 300 nodes were used in the present study.

Due to the eccentric load path, the single lap joint is not at moment equilibrium, if tensile forces are applied parallel to the adherend plates. External moments are required to satisfy the moment equilibrium condition as shown in Fig. 2. In the present analysis aluminium, steel and Boron/epoxy materials are considered for adherends. Table 1 gives the mechanical properties of materials considered for adherends and adhesive layers. Table 2 gives the overall orthotropic properties for angle-ply Boron/epoxy laminate and quasi-isotropic Boron/epoxy laminate.

Figure 4 shows the normal and shear stress distribution in the adhesive layer of aluminium-aluminium single lap joint The finite element solution is found to (adhesive thickness, $t_a = 0.1$mm). The finit solution is found be in good agreement with the closed-form solution of the Goland and Reissner (1944). The normal and shear stresses at the ends of the overlap are found to be the maximum and the

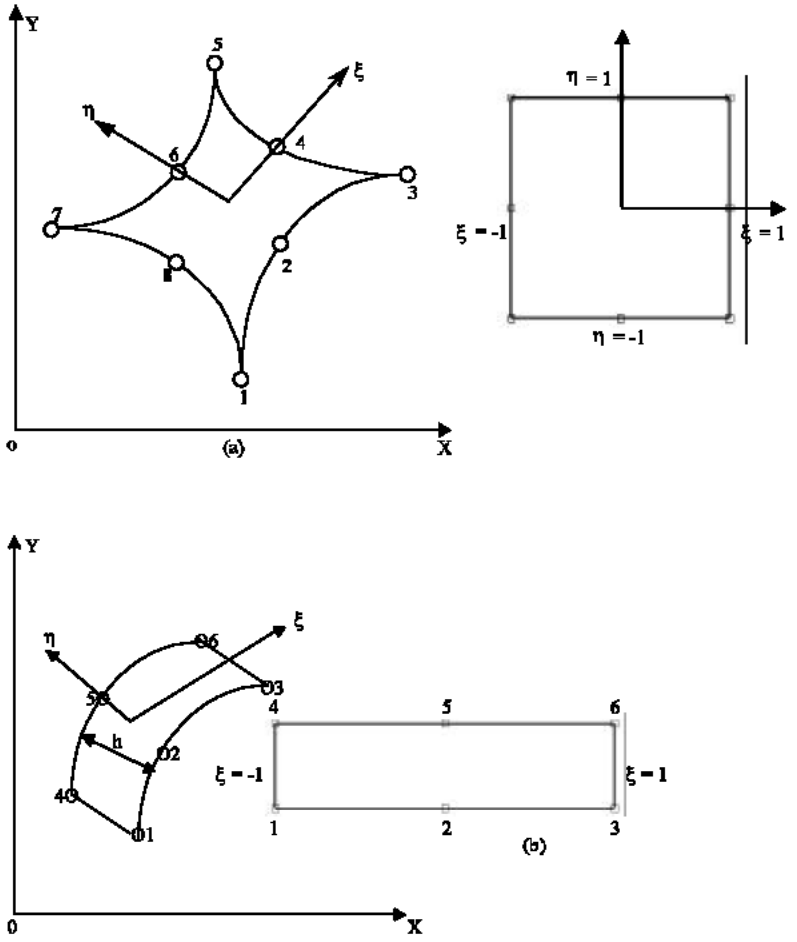

Fig. 2: Quadratic isoparametric elements (a) General element for adherends (b) Special element for adhesive

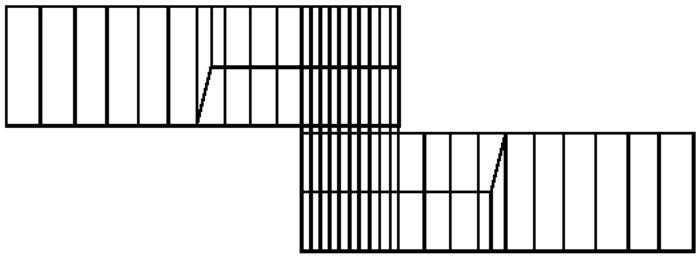

Fig. 3: Finite element idealization of single lap joint

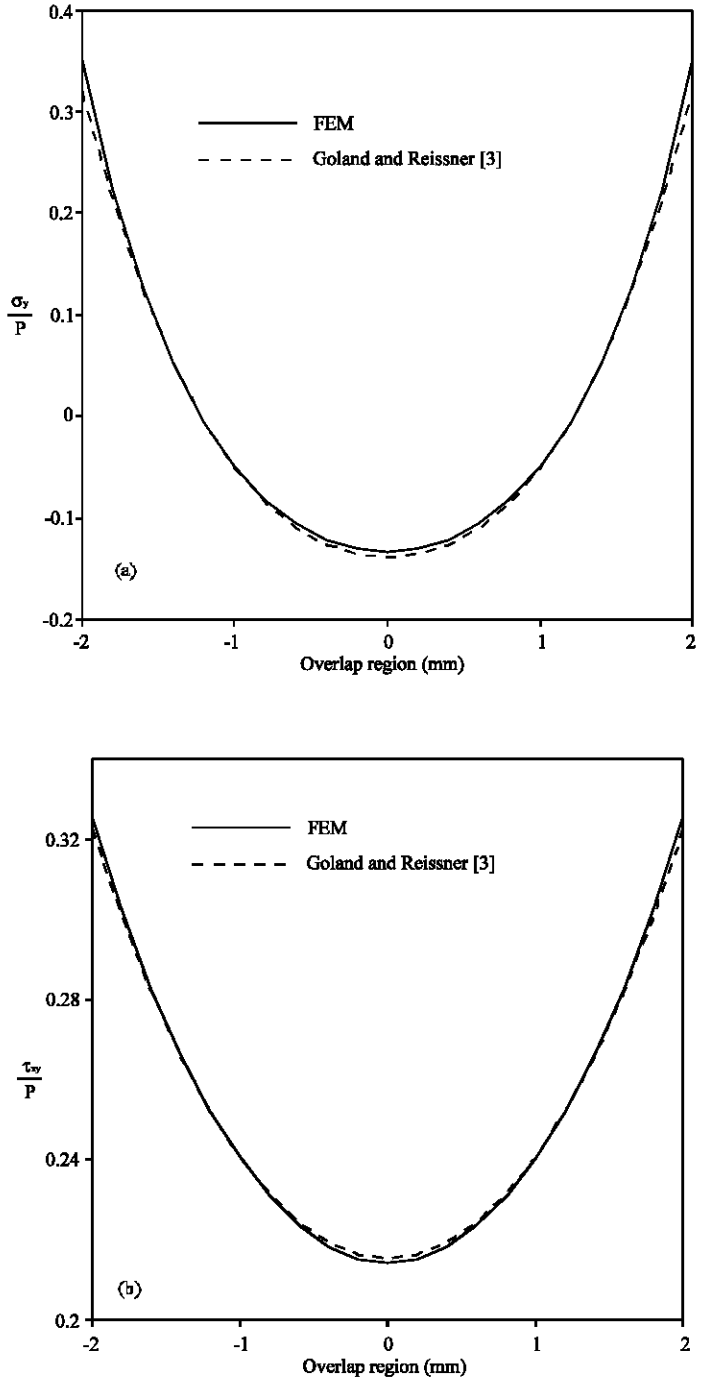

Fig. 4: Normal and shear stress distributions in the adhesive layer of aluminium-aluminium single lap joint (adhesive thickness, $t_a = 0.1$mm)

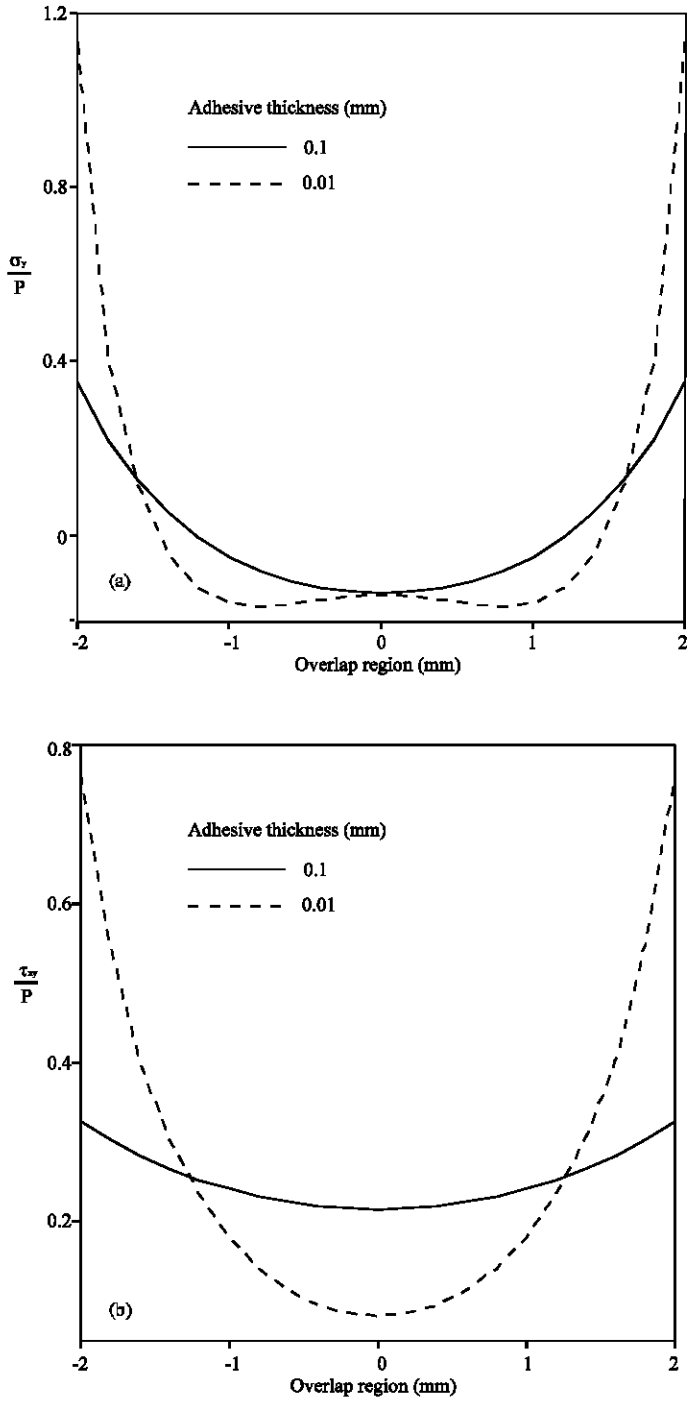

Fig. 5: Normal and shear stress distributions in the adhesive layer of aluminium-aluminium single lap joint with different adhesive thickness

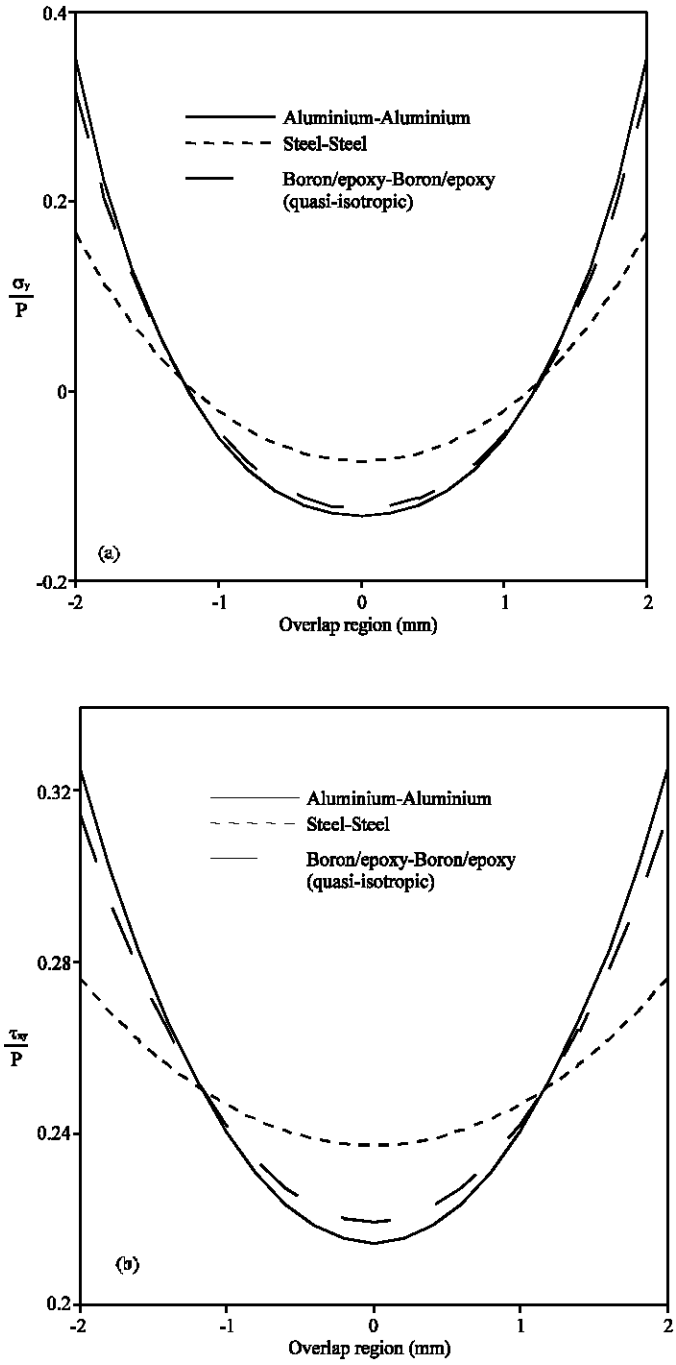

Fig. 6: Comparison of normal and shear stress distributions in the adhesive layer of single lap joints having different adherend materials (adhesive thickness, $t_a = 0.1$mm)

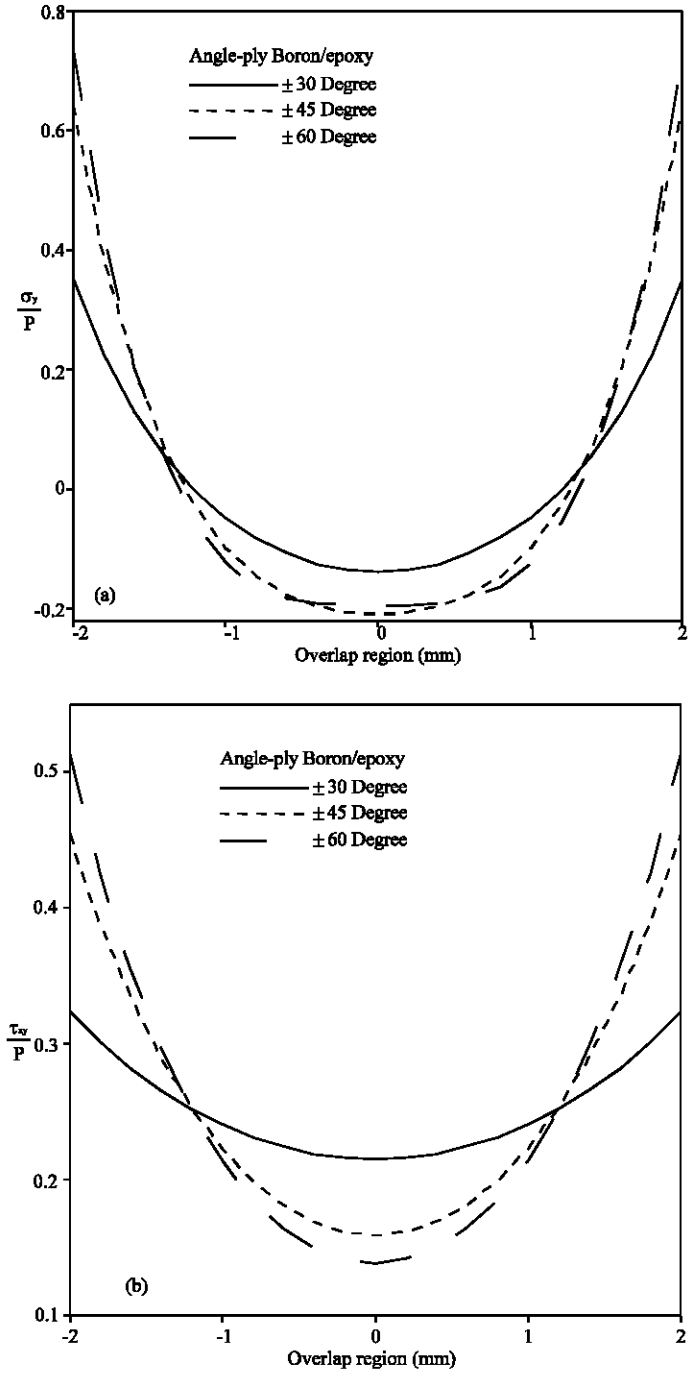

Fig. 7: Comparison of normal and shear stress distributions in the adhesive layer of single lap joint having different angle-ply boron/epoxy adherends (adhesive thickness, $t_a = 0.1$mm)

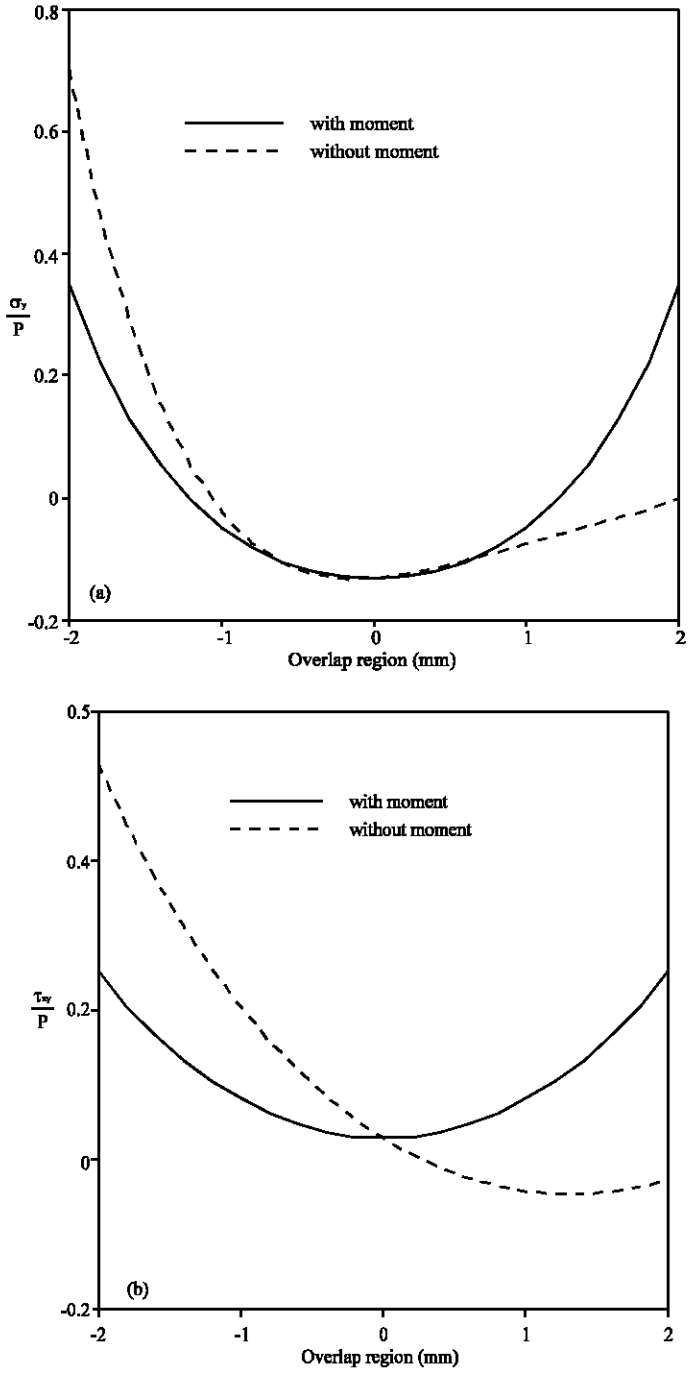

Fig. 8: Comparison of normal and shear stress distributions in the adhesive layer of aluminium - aluminium single lap joint (adhesive thickness, $t_a = 0.1$mm)

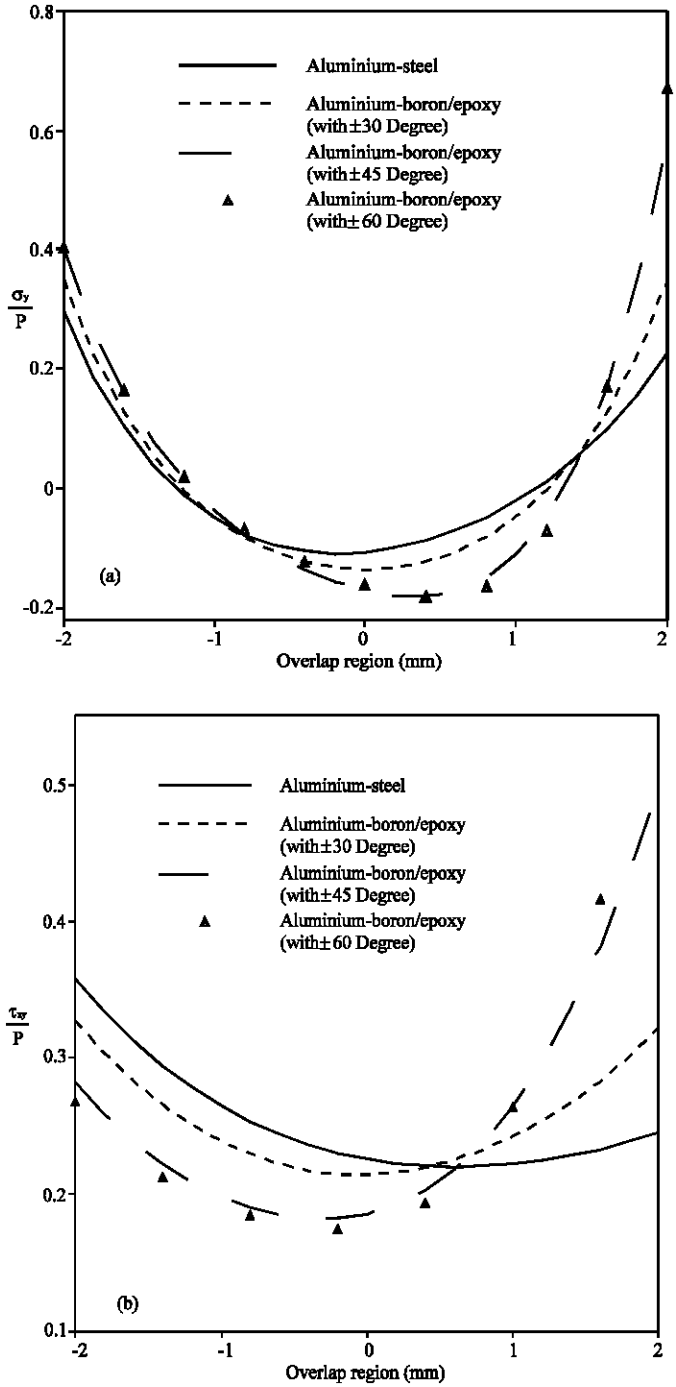

Fig. 9: Comparison of normal and shear stress distributions in the adhesive layer of single lap joint having aluminium adherend connecting with different angle-ply boron/epoxy adherends (adhesive thickness, $t_a = 0.1$ mm)

distribution is symmetric in either side from the centre of the joint. Figure 5 shows the normal and shear stress distributions in the adhesive layer of aluminium - aluminium single lap joint with different adhesive thickness. The results indicate that the normal stress zone tends to become narrow and the peak stress becomes higher as the thickness of the adhesive layer decreases. Figure 6 shows the comparison of normal and shear stress distributions in the adhesive layer of a single lap joint having different adherend materials. Figure 7 shows the comparison of the stress distribution in the adhesive layer of a single lap joint having different angle-ply Boron/epoxy adherends. The normal and shear stress distribution for a single lap joint under the horizontal applied force (without external moment) are shown in Fig. 8. Since the joint undergoes rotation, there is no symmetry as expected in the stress distribution on either side from the center of the joint. Figure 9 shows the comparison of stress distributions in the adhesive layer of single lap joint having aluminium adherend connecting with different angle-ply boron/epoxy adherend. It is very interesting to note that the normal and shear stress distributions for the single lap joints under the horizontal applied force with the external moment showed un-symmetry in the stress distribution on either side from the center of the joint because of different adherend materials.

Conclusions

Accurate finite element stress analysis results can be obtained for complex adhesively bonded joints by modeling them with the six-node special element for adhesive layer and the eight-node iso-parametric quadrilateral element for adherends. By loading the structure in increments and through the use of an iterative procedure, it is possible to extend the linear solution of the elasticity problem into the plastic range. Future work is towards the evaluation of failure load and its validation through experimental results.

References

Barker , R.M. and F. Hatt, 1973. Analysis of bonded joints in Vehicular structures. AIAA J., 11: 1650-1654.

Carpenter W.C., 1989. Goland and Reissner were correct. J. Strain Anal., 24: 185-187.

Chang D.J. and R. Muki 1974. Stress distribution in a lap joint under tension-shear. Intl. J. Solids and Struct., 10: 503-517.

Erdogan, F. and M. Ratwani, 1971. Stress distribution in bonded joints. J. Composite Materials, 5: 378-393.

Goland, M. and E. Reissner 1944. The stresses in cemented joints. J. Applied Mechanics, 11: 17-27.

Hart-Smith, L.J., 1973a. Adhesive-bonded double lap joints. National Aeronautics and Space Administration, Langley Research Center, Hampton, Virginia 23366. Report No. NASA-CR- 112235.

Hart-Smith, L.J., 1973b. Adhesive-bonded single lap joints. National Aeronautics and Space Administration, Langley Research Center, Hampton, Virginia 23366. Report No. NASA-CR- 112236.

Hart-Smith L.J., 1973c. Adhesive-bonded scarf and stepped lap joints. National Aeronautics and Space Administration, Langley Research Center, Hampton, Virginia 23366. Report No. NASA-CR- 112237.

Hart-Smith, L.J., 1974. Analysis and design of advanced composite bonded joints. National Aeronautics and Space Administration, Washington, DC20546. Report No. NASA-CR-2218.

Mathews, F.L. and R.D. Rawlings, 1999. Composite Materials: Engineering and Science. Cambridge, Woodhead.

Mathews, F.L., G.A.O. Davies, D. Hitchings and C. Soutis, 2000. Finite Element Modeling of Composite Materials and Structures. Cambridge England, Woodhead Publishing Limited.

Ramamurthy, T.S. and A.K. Rao, 1978. Shaping of adherends in bonded joints. Intl. J. Mechanical Sci., 20: 721-727.

Reddy, M.N. and P.K. Sinha, 1975. Stresses in adhesive- bonded joints for composites. Fibre Sci. Technol., 8: 33-47.

Yuceoglu, U. and D.P. Updike, 1980. Stress analysis of bonded plates and joints. J. Eng. Mechanics Division, ASCE, 106: 37-56.

Zienkiewicz, O.C., 1971. The Finite Element Method in Engineering Sciences. McGraw-Hill, London.